EFFECT OF DARCY, FLUID RAYLEIGH AND HEAT GENERATION PARAMETERS ON NATURAL CONVECTION IN A POROUS SQUARE ENCLOSURE: A BRINKMAN-EXTENDED DARCY MODEL

S.Das
Mechanical Engineering Department
Regional Engineering College
Rourkela 769 008
Orissa, INDIA

R.K.Sahoo
Mechanical Engineering Department
Regional Engineering College
Rourkela 769 008
Orissa, INDIA

ABSTRACT

A Pressure-velocity solution for natural convection for fluid saturated heat generating porous medium in a square enclosure is analysed by finite element method. The numerical solutions obtained for wide range of fluid Rayleigh number, Ra_f, Darcy number, Da, and heat generating number, Q_d. The justification for taking these non-dimensional parameters independently is to establish the effect of individual parameters on flow patterns. It has been observed that peak temperature occurs at the top central part and weaker velocity prevails near the vertical walls of the enclosure due to the heat generation parameter alone. On comparison, the modified Rayleigh number used by the earlier investigators[4,6], can not explain explicitly the effect of heat generation parameter on natural convection within an enclosure having differentially heated vertical walls. At higher Darcy number, the peak temperature and peak velocity are comparatively more, resulting in better enhancement of heat transfer rate.

Introduction

Analysis of flow and convective heat transfer in volumetrically heated porous layer has become a separate topic for research in the last twenty five years in view of its importance in various engineering applications, such as heat removal from nuclear fuel debris, heat transfer associated with storage of nuclear waste, exothermic reaction in packed-bed reactors, heat recovery from geothermal systems and particularly in the field of large storage systems of agricultural products.

Several studies on convective heat transfer in heat-generating porous media have been reported for different physical formulation and geometric models with various boundary conditions. Gasser et al. [1] studied the onset of convection in a horizontal porous layer, both stabilising and destabilising temperature gradients. Somerton et al. [2] obtained the solution for the case of volumetrically heated porous layer with an adiabatic lower surface and a zero applied temperature gradient. Haajizadeh et al.[3] has presented a Darcy solution for natural convection in a porous enclosure with vertical side wall cooling. Prasad[4] has reported the study of Darcian effect in rectangular cavity with vertical walls which are isothermally cooled. All these investigators have considered a single wall temperature of the enclosure. Later, Prasad et al.[5] have presented solution for natural convection within rectangular enclosure for differentially heated vertical wall temperature with no heat generation. Several studies have also shown the effect of Brinkman extension and Forchheimer formulation of Darcy's equation for flow in porous media. Stewart et al [6] have employed the modified Darcy's equation using Forchheimer formulation to study the non-Darcian effect for enclosures having single boundary wall temperature. One of the objective of the present problem is to investigate the convective flow using Brinkman-extended Darcy's law for wide range of flow parameters. Brinkman-extended Darcy law is chosen to justify the no-slip condition over the solid wall boundaries and also the viscous term in its Navier-Stokes equation. Although Chan et al.[7] inferred that inclusion of viscous term and consequent satisfaction of the no-slip condition, give virtually the same result as a pure Darcy law analysis for lower range of modified Rayleigh number. Furthermore, a very little work has been reported on natural convection within rectangular enclosure filled with heat generating porous media bounded by two vertical isothermal walls at two different temperatures. It has been established that the flow patterns and isotherms exhibit distinctly different behavior in differentially heated vertical cavity than that of single wall temperature. The second objective of the paper is to include the effect of differentially heated vertical isothermal walls which has more practical relevance than that of a single wall temperature.

Physical Model

The physical system under consideration is a square enclosure. The vertical walls of the

enclosure have been considered to be heated isothermally at two different temperatures, while the horizontal walls are perfectly insulated. No-slip condition is chosen throughout the boundary. It is assumed that the porous medium is isotropic, homogeneous and saturated with an incompressible fluid. The thermophysical properties of the fluid and solid matrix are constant except for fluid density variation in the body force term. The viscous dissipation is negligible. Furthermore, the solid particle and fluid are assumed to be in local thermodynamic equilibrium. These assumptions are general and the purpose of the analysis is to provide a basic understanding of flow phenomenon for heat generating, differentially heated porous enclosure.

Thus the governing equations of conservation of mass, momentum and energy for steady flow through the porous medium are given as follows:

$$\frac{\partial u}{\partial x}+\frac{\partial v}{\partial y}=0 \tag{1}$$

$$\frac{1}{\varepsilon^2}\left[u\frac{\partial u}{\partial x}+v\frac{\partial u}{\partial y}\right]=-\frac{\partial p}{\partial x}-\frac{Pr}{Da}u+\frac{Pr}{\varepsilon}\left[\frac{\partial^2 u}{\partial x^2}+\frac{\partial^2 u}{\partial y^2}\right] \tag{2}$$

$$\frac{1}{\varepsilon^2}\left[u\frac{\partial v}{\partial x}+v\frac{\partial v}{\partial y}\right]=-\frac{\partial p}{\partial y}-\frac{Pr}{Da}v+\frac{Pr}{\varepsilon}\left[\frac{\partial^2 v}{\partial x^2}+\frac{\partial^2 v}{\partial y^2}\right]+T.Ra.Pr \tag{3}$$

$$u\frac{\partial T}{\partial x}+v\frac{\partial T}{\partial y}=\frac{\partial}{\partial x}\left[\lambda\frac{\partial T}{\partial x}\right]+\frac{\partial}{\partial y}\left[\lambda\frac{\partial T}{\partial y}\right]+(1-\varepsilon)Q_d \tag{4}$$

In the above equations the variables are reduced to dimensionless form by introduction of the following scales

$$x,y=(x^*,y^*)/L; \qquad u,v=(u^*,v^*)L/\alpha; \qquad p=(p^*L^2)/(\rho\alpha^2);$$

$$T=(T^*-T_c)/(T_h-T_c); \tag{5}$$

The astrics denote dimensional variables. The variables u^* and v^* are the velocity components in x^* and y^* directions, p^* is the pressure and T^* is the temperature. The dimensionless numbers are defined as,

Rayleigh Number, $Ra_f=\dfrac{g\beta_T(T_h-T_c)L^3_{ref}}{\nu_f\alpha_f}$

Prandtl Number, $Pr=\dfrac{\nu_f}{\alpha_f}$

Darcy Number, $Da=\dfrac{\kappa}{L^2_{ref}}$ and

Non-dimensional heat generation number, $Q_d=\dfrac{L^2_{ref}q'''}{\alpha_f(T_h-T_c)\rho_f C_{pf}}$ (6)

The governing equations are scaled on the basis of fluid Rayleigh number as in the case of viscous fluid(independent of permeability) instead of modified Rayleigh number. The scaling has been intended to observe the effect of individual matrix and fluid parameters explicitly.

Finite element method is chosen to predict the various parameters. A suitable grid generation scheme with isoparametric, quadrilateral elements is adopted for stability of numerical results. All the elements are containing eight nodes, one at each corner and one at midpoint of each side. All eight nodes are associated with velocities as well as temperature; where the corner nodes are associated with pressure. This is an accepted practice given by Taylor et al. [8] for depicting the variation in pressure by shape function M_l, of one order less than those shape function N_j defined for velocities and temperature.

$$u = \sum_{j=1}^{8} N_j u_j \qquad v = \sum_{j=1}^{8} N_j v_j$$

$$T = \sum_{j=1}^{8} N_j T_j \qquad p = \sum_{l=1}^{4} M_l p_l \tag{7}$$

By employing the Galerkin weighted residual approach and substituting the spatial variation of u,p,v and T given by eq. (7) in eqs. (1)-(4) following set of algebraic equations are obtained.

$$\sum_{l}^{n^e} \int_{A^e} M_l \left[\frac{\partial N_j}{\partial x} u_j + \frac{\partial N_j}{\partial y} v_j \right] dA^e = 0 \tag{8}$$

$$\sum_{l}^{n^e} \int_{A^e} \left[\frac{1}{\varepsilon^2} N_i N_k u_k \frac{\partial N_j}{\partial x} u_j + \frac{1}{\varepsilon^2} N_i N_k v_k \frac{\partial N_j}{\partial y} u_j + N_i \frac{\partial M_l}{\partial x} p_l + \frac{Pr}{Da} N_i N_j u_j + \right.$$
$$\left. + \frac{Pr}{\varepsilon} \left[\frac{\partial N_i}{\partial x} \frac{\partial Nj}{\partial x} u_j + \frac{\partial N_i}{\partial y} \frac{\partial Nj}{\partial y} u_j \right] \right] dA^e = \int_{\Gamma} \frac{1}{\varepsilon} Pr N_i \frac{\partial u}{\partial n} d\Gamma \tag{9}$$

$$\sum_{l}^{n^e} \int_{A^e} \left[\frac{1}{\varepsilon^2} N_i N_k u_k \frac{\partial N_j}{\partial x} v_j + \frac{1}{\varepsilon^2} N_i N_k v_k \frac{\partial N_j}{\partial y} v_j + N_i \frac{\partial M_l}{\partial y} p_l + \frac{Pr}{Da} N_i N_j v_j + \right.$$
$$\left. + \frac{Pr}{\varepsilon} \left[\frac{\partial N_i}{\partial x} \frac{\partial Nj}{\partial x} v_j + \frac{\partial N_i}{\partial y} \frac{\partial Nj}{\partial y} v_j \right] - Ra\, Pr\, N_j T_j \right] dA^e = \int_{\Gamma} \frac{1}{\varepsilon} Pr N_i \frac{\partial v}{\partial n} d\Gamma \tag{10}$$

$$\sum_{l}^{n^e} \int_{A^e} \left[N_i N_k u_k \frac{\partial N_j}{\partial x} T_j + N_i N_k v_k \frac{\partial N_j}{\partial y} T_j + \lambda \left[\frac{\partial N_i}{\partial x} \frac{\partial N_j}{\partial x} T_j + \frac{\partial N_i}{\partial y} \frac{\partial N_j}{\partial y} T_j \right] \right.$$
$$\left. (1-\varepsilon) Q_d \right] dA^e = -\int_{\Gamma} N_i \frac{\partial T}{\partial n} d\Gamma \tag{11}$$

The indices i, j, k=1....8; and l=1....4;

The above eqs. (8)-(11) are discretised form of governing equations in primitive variable formulation in u,p,v and T. As the coefficient matrix of these set of equations is sparse in nature with very high order, a suitable technique is necessary in order to reduce the computation time and memory. In the present text frontal technique[9] is used which requires a suitable element numbering scheme in order to reduce the front width. An iterative scheme is adopted with initial guess values of u and v till the desired convergence in the tolerance of 10^{-3} is obtained.

Results and Discussion

The numerical results are obtained for an enclosure filled with heat generating saturated porous medium. The enclosure is having differentially heated two vertical isothermal walls and two horizontal adiabatic walls. For the sake of analysis, aspect ratio of the enclosure is taken to be unity and Prandtl number, Pr = 1. The range of other parameters considered here are Darcy number($10^{-6} \leq Da \leq 10^{-2}$), fluid Rayleigh number ($10^3 \leq Ra_f \leq 10^7$) and heat generation number Q_d ($1 \leq Q_d \leq 10^3$). The porosity, ε of the medium is taken to be 0.4 and 0.2 for the sake of comparison. The justification of present dimensionless analysis is to study the effect of porous matrix scaling parameters Da, ε, and Q_d and fluid scaling parameter Ra_f on heat transfer and fluid flow characteristics.

At very low Darcy number and low rate of heat generation, (Da = 10^{-6}, Q_d=1), pure heat conduction dominates even at Rayleigh number of the order 10^7. In such condition, flow remains always unicellular and the isothermal lines at central region remain more horizontal. As Rayleigh number increases lateral conduction predominates only in the thin boundary layer of the wall. This conclusion is satisfactorily explained in the case of enclosure without porous medium. However it is obvious that pure heat conduction will prevail at some higher range of Rayleigh number due to the presence of porous medium.

The isothermal lines and streamlines patterns are plotted for Da at 10^{-4} and 10^{-2}. At each of these Da, Q_d is taken to be 10 and 10^2 and Ra_f is taken to be 10^5 and 10^6. These results are plotted at porosity 0.4 and 0.2 as shown in fig. 1.

Without heat generation, the maximum temperature occurs at the hot wall. This temperature increases and drifts towards the center of top wall with the increasing Q_d as shown in fig.1. This is due to the fact that the hot fluid reaching the top left corner of the enclosure is unable to reject energy since the velocities are small. The u-velocity along the mid vertical height shows clearly the fall of velocity at the top region as compared to that of bottom as shown in Fig. 2. Increasing Ra_f alone at moderate range ($Ra_f \leq 10^5$) does not effect the peak temperature appreciably. The earlier work[4], where modified Rayleigh

number is used alone, may not be able to explain the flow pattern without these individual parameters (Ra_f, Da and Q_d) used here.

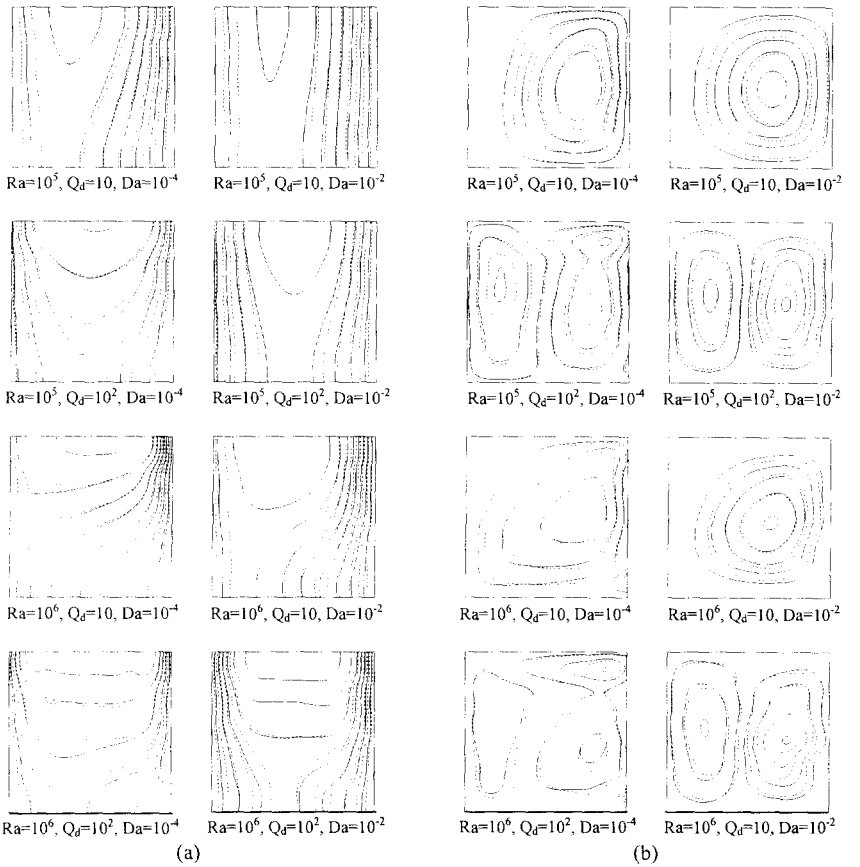

FIG. 1
Flow patterns for different range of parameters (a) Isotherms; (b) streamlines; with porosity, $\varepsilon = 0.4$(continuous line) and $\varepsilon = 0.2$ (dashed line)

Another important result is to be noted that fluid having higher heat generation rate will induce a weaker vorticity even at a very low Ra_f and thus it gives rise to a bicellular structure as shown in fig. 1(b). But the symmetricity of this bicellular structure does not exist due to effect of differentially heated vertical walls which is in contrast to those work with single boundary wall temperature. The v-velocity along the mid horizontal axis is plotted to confirm the coexistence of bicellular structure as shown in fig. 2(b). This unsymmetric bicellular flow is also apparent from the streamline plots. However, at very high heat generation rate, the core flow is distorted to an extent to produce multicellular structures within the domain. In Brinkman's model the velocity is zero at the wall, increasing to a peak value, and then

dropping to zero in the core region. As the value of Da increases, the position of the peak velocity shift away from wall as shown in fig. 2. For a given model the flow intensity and thermal activity increases

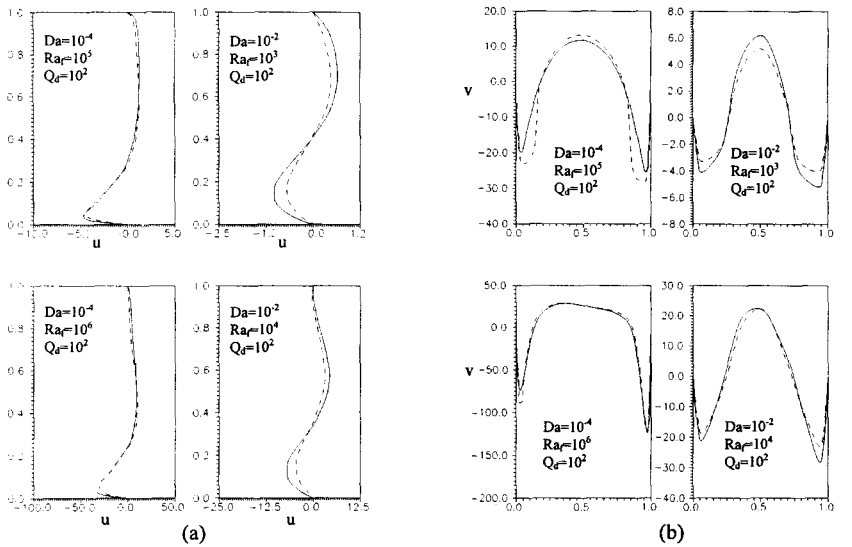

FIG.2

Velocity plot (a) u-velocity at mid vertical height; (b) v-velocity at mid horizonatal height; with porosity, ε=0.4(continuous line) and ε=0.2(dashed line).

with the increasing Darcy number since the permeability of the system has increased, thereby reducing the resistance to flow.

Figure 3 shows the contour plots of dimensionless u and v velocities with increase in Darcy and Rayleigh numbers. Although the u and v at the mid axes is given in fig. 2, it is more interesting to see the general nature of u and v variation inside the domain as shown in fig. 3 for certain flow parameters. This figure clearly indicates change of flow pattern from unicellular to bicellular where the symmetric structure of the core is never sustained.

The above problem is also extended to study the effect of change of porosity on convective flow patterns. It has been observed that increase in porosity of the medium is found to have significant effect on peak temperature as well as peak velocities. Because there is an overall reduction in damping resistance offered by porous matrix which leads to higher velocity and this in turn results steeper temperature gradient and large Nusselt number at higher porosity.

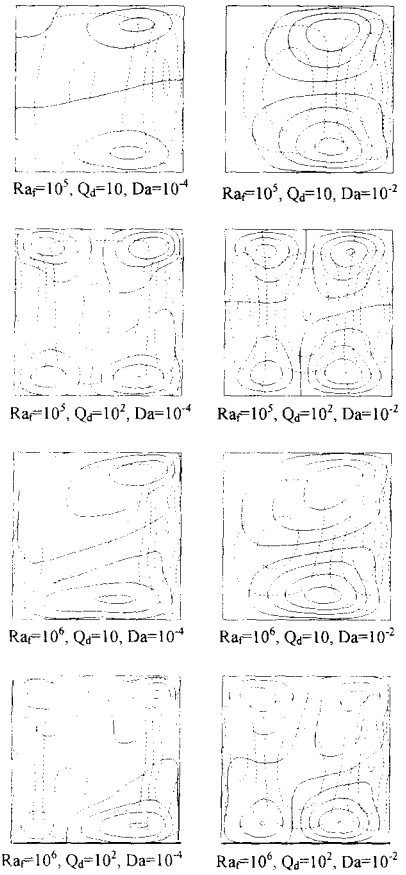

Fig. 3
Velocity contour plot, u-velocity(continuous line); v-velocity(dashed line); with porosity $\varepsilon=0.4$

Acknowledgments

The present investigation was carried out under the partial support from Grant No. F 8017/RDII/BOR/95, AICTE, Government of India.

Nomenclature

A^e	Area of an element,
C_{pf}	Specific heat of fluid,
Da	Darcy number,

g	Gravitational constant, (m/s^2)
L_{ref}	Characteristic length; (m)
M,N	Shape function;
Q_d	Heat generation number;$(L^2_{ref} \cdot q''' / \alpha_f (T_h - T_c)\rho_f C_{pf})$
q'''	Uniform heat generation rate per unit volume,
n^e	Number of elements,
p	Dimensionless fluid pressure,
Pr	Prandtl number; ν_f/α_f
Ra_f	Rayleigh number; $g\beta_T (T_h - T_c)L^3_{ref} / \nu_f \alpha_f$
T	Non-dimensional temperature, $(T-T_c)/(T_h-T_c)$
T_h, T_c	Temperature of hot wall,
u,v	Dimensionless velocities,
x,y	Dimensionless co-ordinates,
Greek	Symbols
α_f	Fluid thermal diffusivity,
β_T	Coefficient of thermal expansion,
Γ	Length of boundary,
κ	Permeability ratio,
λ	Conductivity ratio,
ε	Porosity,
ρ_f	Fluid density,
ν_f	Fluid kinematics viscosity,

References

1. R.D. Gasser, and M.S. Kazimi, Onset of Convection in a Porous Medium and Internal Heat Generation, J. Heat Transfer, vol. 98, pp. 48-54 (1976).

2. C.W. Somerton, J.M. McDonough and I. Catton, Natural Convection in a Volumetrically heated Porous Layer, Winter Annual Meeting of A.S.M.E. HTs-Vol. 22, Heat Transfer in Porous Media, Phoenix, Arizona, pp. 43-47, (1982).

3. M. Haajizadeh, A.F. Ozgue, and C.L. Tien, Natural Convection in a Vertical Porous Enclosure With Internal Heat Generation, Int. J. Heat Mass Transfer, Vol. 27, no. 10, pp. 1893-1902, (1984).

4. V. Prasad, Thermal Convection in a Rectangular Cavity With a Heat-Generating Darcy Porous Medium, Journal of Heat Transfer, A.S.M.E., vol. 109, pp. 697-703 (1987).

5. V. Prasad, and N. Kladias, Natural Convection in Horizontal Porous Layers: Effects of Darcy and Prandtl Numbers, Transactions of the ASME, Journal of Heat Transfer, vol.111, pp. 926-935 (1989).

6. W.E. Stewart Jr., L. Cai and L.A. Stickler, Convection in Heat-Generating Porous Media With Permeable Boundary Natural Ventilation of Grain Storage Bins, Transactions of A.S.M.E, Journal of Heat Transfer, vol. 110, pp. 1044-1046 (1994).

7. B.K.C. Chan, C.M. Ivey and J.M. Barry, Natural Convection in Enclosed Porous Media With Rectangular Boundaries, J. Heat Transfer, vol. 92, pp. 21-27 (1970).

8. C. Taylor, and P. Hood, A Numerical Solution of Navier-Stokes Equation Using the Finite Element Technique. Computer and Fluid vol. 1, pp. 73-100 (1973).

9. S.W. Sloan, A Frontal Program for Profile and Wavefront Reduction, Int. J. for Numerical Method in Engineering, vol. 28, pp. 2651-2679 (1989).